PERFORMANCE ANALYSIS OF A PV POWERED DC MOTOR DRIVING A 3-PHASE SELF-EXCITED INDUCTION GENERATOR

S. M. Alghuwainem
E.E. Department, King Saud University
Riyadh, Saudi Arabia 11421

ABSTRACT

Photovoltaic (PV) powered dc motors driving dedicated loads (e.g. water pumps) are increasingly used in the remote rural areas of many developing countries. The key to their success is simplicity (direct coupling, no dc-ac inversion, no storage batteries, etc.). In this paper a PV powered dc motor is used to drive an isolated three-phase self-excited induction generator (SEIG). It is found that due to the unique torque-speed characteristics of the SEIG, utilization efficiency is close to maximum at all insolation levels with no peak-power tracking. The proposed arrangement is useful as part of an integrated renewable energy system (IRES), which takes advantage of the inherent diversity of wind and insolation in most developing countries to improve power quality. The SEIG is driven by wind turbine, dc motor, or both. Performance of the system under different insolation conditions is analyzed.

Keywords: - Photovoltaic generators; solar cells; dc motors; induction generators; integrated renewable energy systems.

INTRODUCTION

Utilities in many developing countries are finding it difficult to establish and maintain remote rural area electrification. The cost of delivering power to such areas is becoming excessively large due to large investments in transmission lines or locally installed capacities, and large transmission line losses. For these reasons, many utilities are seriously considering local renewable energy resources, mainly wind and PV, as alternatives for supplying energy to rural remote areas. In many developing countries, wind and insolation are complementary over the annual cycle [1]. It is therefore desirable to take advantage of this inherent diversity by combining PV and wind systems into one integrated renewable energy system (IRES). In addition to minimizing the overall system cost by sharing some of the equipment, the IRES improves power quality and minimizes the need for energy storage.

95 SM 462-2 EC A paper recommended and approved by the IEEE Energy Development and Power Generation Committee of the IEEE Power Engineering Society for presentation at the 1995 IEEE/PES Summer Meeting, July 23-27, 1995, Portland, OR. Manuscript submitted December 29, 1993; made available for printing June 5, 1995

The squirrel-cage self-excited three-phase induction generator (SEIG) has been used for many years to convert wind power to electrical power. Due to its simplicity, ruggedness, and low cost, it provides a reliable and relatively inexpensive means to convert mechanical wind power to three-phase electrical power over a wide range of rotor speeds for loads where frequency and voltage need not be regulated. Over the past decade, many researchers have investigated the steady-state performance of the SEIG [2-4]. References [5-7] evaluate the excitation capacitance requirements of the SEIG under different load and speed conditions.

PV generators convert solar energy to dc electrical power, which may be used directly by some loads where energy is stored in batteries or converted to ac power using dc-ac inverter. Inverter control equipment, peak power trackers, harmonic filters, and protection devices are all incorporated with the inverter in one unit called power conditioning unit (PCU). The cost of PCU, efficiency, and reliability, are important factors to consider when opting for dc-ac inversion. The simplest and least expensive means to convert PV power to mechanical power is to use it to drive a dc motor. In order to avoid additional costs, the motor is directly coupled to the PV generator without storage batteries. This arrangement is typically used on noncritical loads such as water pumps, which need not operate continuously and water can be used directly or stored easily. With the increased use of these systems, more attention is paid to their design and optimum utilization in order to achieve the most reliable and economical operation. Because of the relatively high cost of a PV generator, the system designer is interested in its full utilization by optimum matching of the dc motor and its mechanical load to the PV generator so that maximum utilization efficiency is achieved.

In this paper a dc motor is used to drive a three-phase squirrel-cage self excited induction generator (SEIG). The system consists of three different devices; the PV generator, the dc motor, and the induction generator. Each device has its own operating characteristics which is the volt-ampere characteristics for the PV generator and the dc motor, and the torque-speed characteristics for the induction generator. The dc motor drives the induction generator whose torque requirements depend on its electrical load, exciting capacitor, and

speed. The dc motor is supplied from the PV generator whose volt-ampere characteristics depend on the solar insolation variations and on the current drawn by the dc motor. There is a unique point on the volt-ampere characteristics at which power output from the PV generator is maximum, and for optimum utilization the equilibrium operating point must coincide with this point. However, since the maximum power point varies with insolation it is, in general, difficult to maintain optimum matching at all insolation levels.

In order to correct this problem, two options are generally available to the system designer. A) Carefully select the dc motor type and its mechanical load so that they match as closely as possible the maximum power line of the PV generator, or B) Use an electronic control device known as a peak-power tracker (PPT), which continuously matches the output characteristics of the PV generator to the input characteristics of the dc motor. Option (A) offers a compromise matching which is valid only for some solar insolation levels due to drifting of the maximum power point with insolation variations. Reference [8] is a comprehensive study of the starting and steady-state performance of several types of PV powered dc motors driving several types of water pumps. In [9], matching of dc motors to PV generators for maximum daily gross mechanical energy is reported. Reference [10] deals with the operation of loads powered by separate or a common PV source. In [11], the operation of permanent-magnet dc motors driving different types of water pumps and powered by a common PV generator is investigated. Peak-power tracking (option B) is achieved either by discretely interchanging the series-parallel connections of solar cell modules within the PV array [12], or by using a controlled dc-dc converter to adjust the voltage and current levels [13-16].

OPERATION WITH DIRECT COUPLING

The motor is connected directly to the terminals of the PV generator as shown in Fig. 1. Each device has its own characteristics with a unique operating point at which performance is optimum. Therefore for optimum performance of the overall system, the equilibrium operating point must coincide with the point of optimum performance for each device. In order to analyze the performance of the whole system, it is necessary determine the characteristics of the individual devices.

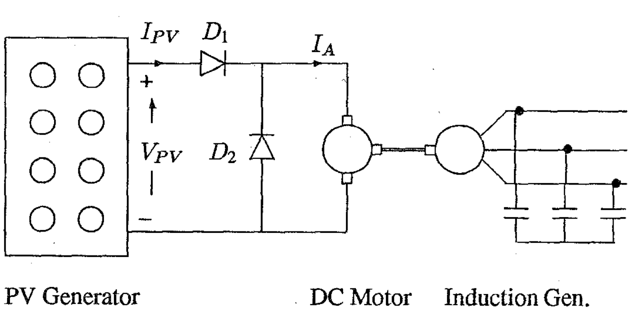

Fig. 1 Operation With Direct Coupling

CHARACTERISTICS OF THE SEIG

The SEIG is actually an induction motor that is driven by a prime mover while its stator excitation is provided by an external capacitor connected to the stator. Because the SEIG is isolated, its stator frequency is free to vary with the rotor speed and the operating slip remains small and negative. Fig. 2 shows the per-phase equivalent circuit commonly used for the steady-state analysis of the three-phase self-excited induction generator [2].

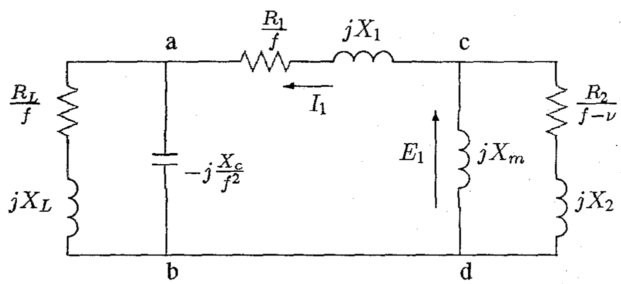

Fig. 2 Per-phase equivalent circuit of self-excited induction generator

The circuit has been transformed to the base frequency (60 Hz.) by introducing the parameters f and ν, where f is the per-unit frequency and ν is the speed in per-unit of the synchronous speed.

The total current at node c may be written as

$$E_1(Y_{cb} + Y_m + Y_{cd}) = 0 \tag{1}$$

Therefore, for successful voltage build-up the total admittance must be zero, since $E_1 \neq 0$.

$$Y_{cb} + Y_m + Y_{cd} = 0 \tag{2}$$

where

$$\begin{aligned} Y_{cb} &= \frac{1}{R_{ab} + R_1/f + j(X_{ab} + X_1)} \\ &= (R_{ab} + R_1/f - j(X_{ab} + X_1))/D \quad (3) \\ D &= (R_{ab} + R_1/f)^2 + (X_{ab} + X_1)^2 \quad (4) \end{aligned}$$

$$R_{ab} = \frac{R_L X_c^2}{f^3 R_L^2 + f(f^2 X_L - X_c)^2} \tag{5}$$

$$X_{ab} = \frac{-X_c(R_L^2 + f^2 X_L^2 - X_L X_c)}{f^2 R_L^2 + (f^2 X_L - X_c)^2} \tag{6}$$

Equating the real and imaginary parts of equation (2) to zero, we have

$$\frac{R_{ab} + R_1/f}{D} + \frac{\frac{R_2}{f-\nu}}{(\frac{R_2}{f-\nu})^2 + X_2^2} = 0 \tag{7}$$

$$\frac{X_{ab} + X1}{D} + \frac{1}{X_m} + \frac{X_2}{(\frac{R_2}{f-\nu})^2 + X_2^2} = 0 \tag{8}$$

Equation (7) is solved for f which is substituted in (8) to obtain X_m. The air-gap voltage E_1 is determined from the magnetization curve which is a plot of E_1 versus X_m.

In this paper, the induction machine used is a 3-phase, 4-pole, 60 Hz, 380 V, 1.0 kW, star-connected, squirrel-cage whose per-phase equivalent circuit parameters in per unit are as follows: $R_1 = 0.1, X_1 = 0.2, R_2 = 0.06, X_2 = 0.2$. The air gap voltage E_1 is expressed in terms of X_m by a piecewise linearized equation of the form:

$$\begin{aligned} E_1 &= 1.2 - 0.2X_m & X_m &\leq 2 \\ E_1 &= 2.4 - 0.8X_m & 2 \leq X_m &\leq 3 \\ E_1 &= 0 & X_m &\geq 3 \end{aligned} \quad (9)$$

A stable operating point exists, provided that X_m is less than the unsaturated value (3 p.u.). Having determined all constants including X_m and E_1, the equivalent circuit of Fig. 2 is completely solved for the steady-state performance of the induction generator. The electrical torque is given by

$$T_{IG} = \frac{3|I_2|^2 R_2}{f - \nu} \quad (10)$$

where

$$I_2 = \frac{E_1}{R_2/(f-\nu) + jX_2} \quad (11)$$

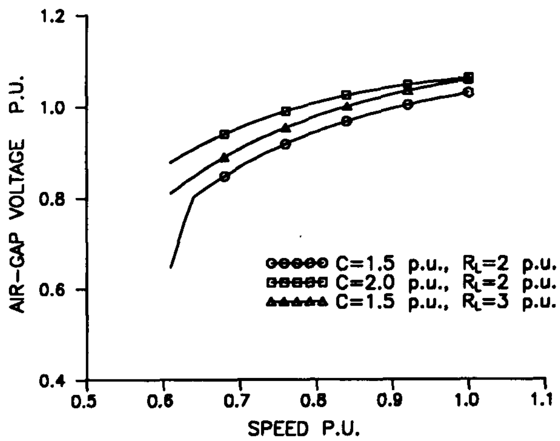

Fig. 3 Air-Gap Voltage Versus Speed

Figs. 3 is a plots of the air-gap voltage, which shows an increases in voltage with increase in speed. Starting with small value of the load resistance R_L, the air-gap voltage first increases rapidly and then slowly as the speed increases.

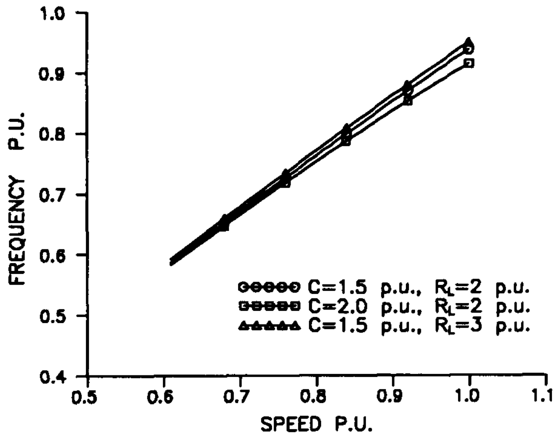

Fig. 4 Frequency Versus Speed

Because the SEIG is isolated, its stator frequency is free to vary with the rotor speed. This is indicated by Fig. 4 which shows that the values of the exciting capacitor and load resistance have negligible effects on the system frequency.

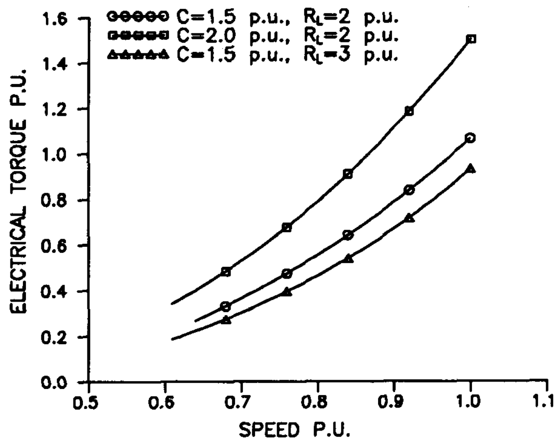

Fig. 5 Electrical Torque Versus Speed

The electrical torque increases with speed as shown in Fig. 5. This relationship is of the form

$$T = k\omega^n \quad \text{, k is constant, and} n \approx 3 \quad (12)$$

The electrical torque increases as the value of the exciting capacitor is increased, but it also increases the negative slip at the same speed (Fig. 6) which degrades efficiency of operation.

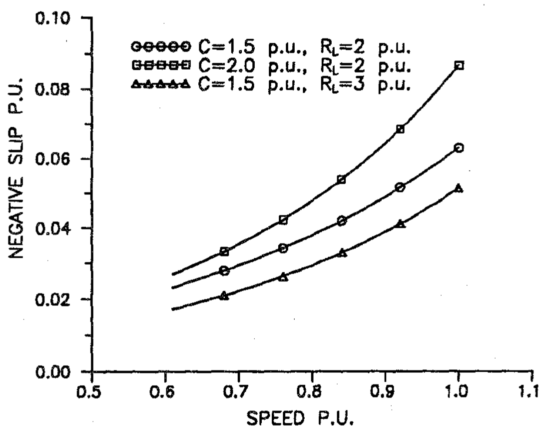

Fig. 6 Negative Slip Versus Speed

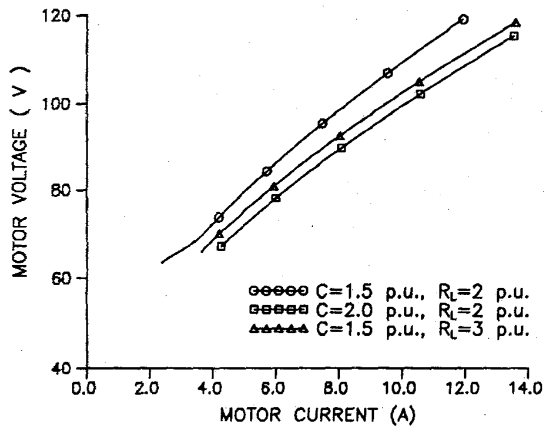

Fig. 7 DC Motor V-I Characteristics

The negative slip variation with speed is shown in Fig. 6. The slip remains small which results in high efficiency. In order to keep frequency at full load small, the exciting capacitor must be kept close to the minimum requirement for self excitation.

CHARACTERISTICS OF THE DC MOTOR

The dc motor used in this study have the following parameters:

Motor type	Permanent Magnet	
Rated voltage	120 V.	
Rated current	13.2 A.	
Rated speed	$\omega = 188.5$ rad./sec.	
Armature resistance	$R_A = 1.9\ \Omega$.	
Mutual Inductance	$M_{AF} = 0.513$ H.	
Armature reaction	Neglected.	
Iron losses	Neglected.	
Rotational losses	$T_L = 0.2 + 0.0015\,\omega$	N-m.

The steady-state voltage, current, speed, and torque are given by

$$V_A = M_{AF}\,\omega + R_A\,I_A \tag{13}$$

$$T_M = M_{AF}\,I_A = T_{IG} + T_L \tag{14}$$

where T_{IG} is the electrical torque of the induction generator, and T_L accounts for total system rotational losses.

The torque applied to the shaft of the dc motor is equal to the electrical torque of the induction generator plus the torque necessary to overcome rotational losses. The electrical torque of induction generator as function of shaft speed is shown in Fig. 5. The corresponding dc motor current and voltage are evaluated at each speed. Fig. 7 is a plot of the volt-ampere characteristics of the dc motor.

CHARACTERISTICS OF THE PV GENERATOR

A PV generator consists of an array of PV modules connected in series-parallel combinations to provide the desired dc voltage and current. The overall volt-ampere characteristics of the array depend on the number of cells in series and the number of parallel strings. The PV generator used in this study consists of 18 parallel strings, 324 cells in series per string, such that the overall volt-ampere characteristic is given by

$$V_{PV} = 23.68\ \ln\left(\frac{I_{PH} - I_{PV} + 0.009}{0.009}\right) - 0.9\ I_{PV} \tag{15}$$

where V_{PV} and I_{PV} are the terminal voltage and current. The photocurrent I_{PH} is directly proportional to insolation, $I_{PH} =$ 14.4 A., at 100 % insolation (1 kW/m^2). Fig 8 is a plot of equation (15) for various insolation levels.

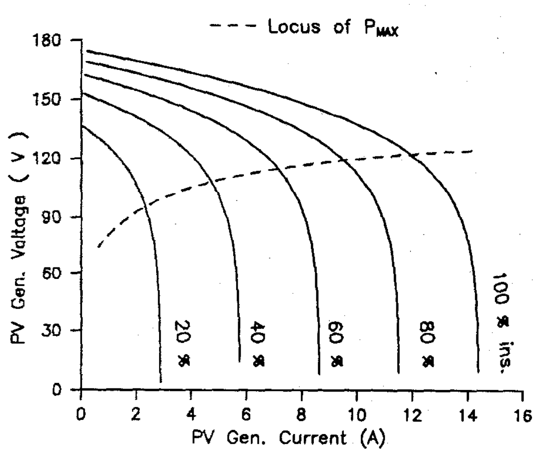

Fig. 8 V-I Characteristic of the PV Generator

The locus of all maximum power points is indicated by the dashed line in Fig. 8. For maximum utilization efficiency of the PV generator, the operating point must follow this locus as the insolation varies. Most loads, however, have their own V-I characteristics and the common operating point may follow a different locus which may be far away from the maximum power locus. In this case matching is necessary to move the operating line as close as possible to the maximum power locus.

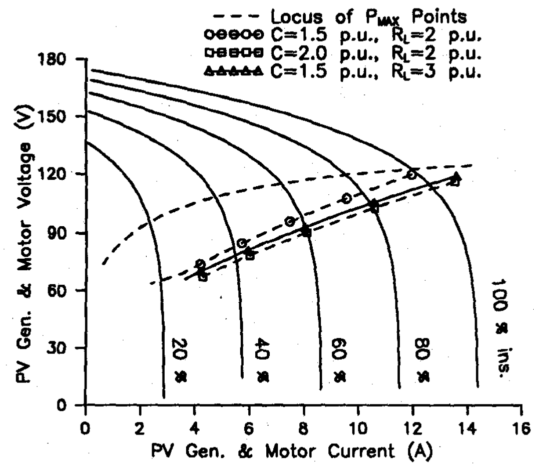

Fig. 9 Common V-I Characteristics

With direct coupling of the dc motor to the PV generator, voltage and current of the two devices are equal, hence the equilibrium operating point is given by the intersection of the two $V-I$ characteristics as shown in Fig. 9. The operating line is close to the maximum power locus line at almost all insolation levels. In order to avoid additional costs, no matching devices or peak-power trackers are necessary. It is also noted that the operating line approaches the maximum power line as the insolation increases.

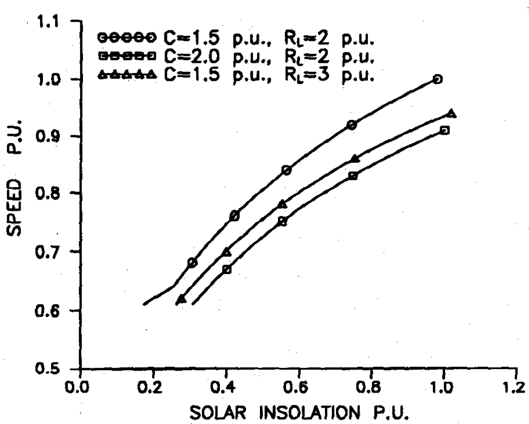

Fig. 10 Speed Versus Insolation

The shaft speed increases with insolation, as shown in Fig. 10. which also shows the effect of the exciting capacitor C, and the load resistance R_L on the system speed as the insolation varies.

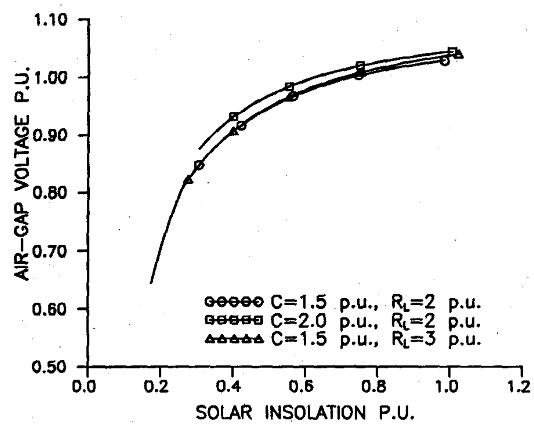

Fig. 11 Air-Gap Voltage Versus Insolation

Fig. 11 is a plot of the air-gap voltage variation with insolation. The voltage builds up rapidly as the insolation increases form a low values and then slowly as the insolation reaches higher levels. It is also seen from Fig. 11 that the rate of the air-gap build up is almost independent of C and R_L.

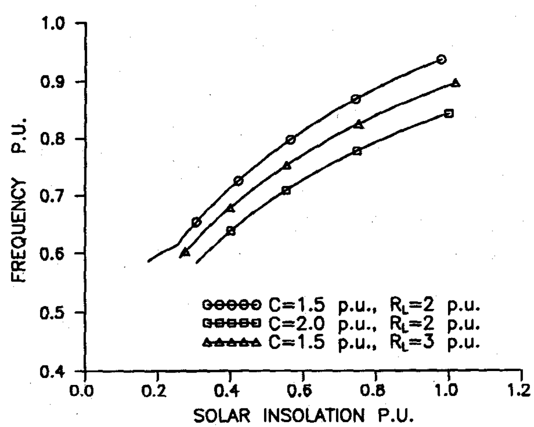

Fig. 12 Frequency Versus Insolation

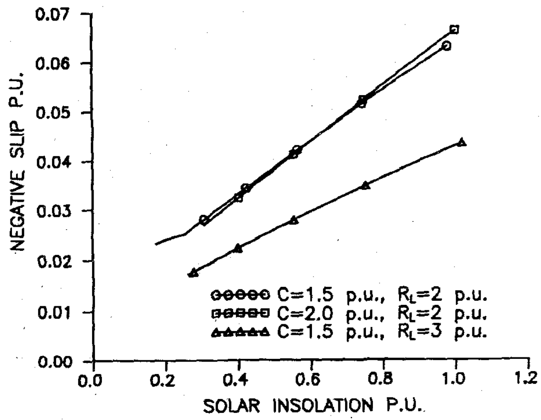

Fig. 13 Slip Versus Insolation

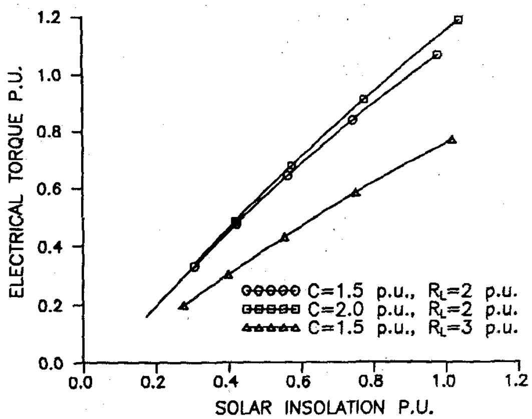

Fig. 14 Electrical Torque Versus Insolation

CONCLUSIONS

Steady-state performance of a PV powered dc motor driving a three-phase SEIG is investigated. It is found that the SEIG represents an almost perfect load match for the PV powered dc motor as far as matching to the PV generator for maximum utilization efficiency is concerned. This eliminates the need for matching devices or peak power trackers which would add to the cost of the system considerably. The proposed arrangement provides a simple, relatively inexpensive, and reliable alternative for supplying three phase power to the rural remote areas of the developing countries. It can be readily used as part of an integrated renewable energy system (IRES) in which an SEIG is driven by the wind turbine, the PV powered dc motor, or both. In many developing countries wind energy and solar energy are complementary to each other over the annual cycle. The IRES can be designed to take advantage of this inherent diversity to improve power quality and minimize energy storage requirements.

REFERENCES

[1] R. Ramakumar, "Renewable energy sources and developing countries," *IEEE Trans. Power Apparatus Syst.*, vol. PAS-102, no. 2, pp. 502-510, Feb. 1983.

[2] S.S. Murthy, O.P. Malik, and A.K Tandon, "Analysis of self-excited induction generators," *IEE Proceedings*, vol. 129, Pt. C, no. 6, pp. 260-265, Nov. 1982.

[3] L. Ouazene and G. McPherson, Jr., "Analysis of the isolated induction generator," *IEEE Trans. Power Apparatus Syst.*, vol. PAS-102, no. 8, pp. 2793-2798, Aug. 1983.

[4] N.H. Malik and S.E. Hague, "Steady state analysis and performance of an isolated self-excited induction generator," *IEEE Trans. on Energy Conversion*, vol. EC-1, no. 3, pp. 134-139, Sep. 1986.

[5] N.H. Malik and A.H. Al-Bahrani, "Influence of the terminal capacitor on the performance characteristics of a self excited induction generator," *IEE Proceedings*, vol. 137, Pt. C, no. 2, pp. 168-173, Mar. 1990.

[6] A.K. Al Jabri and A.I. Alolah, "Limits on the performance of of three-phase induction generators," *IEEE Trans. on Energy Conversion*, vol. EC-5, no. 2, pp. 350-356, June 1990.

[7] T.F. Chan, "Capacitance requirements of self-excited induction generators," *IEEE Trans. on Energy Conversion*, vol. EC-8, no. 2, pp. 304-311, June 1993.

[8] J. Appelbaum, "Starting and steady-state characteristics of dc motors powered by solar cell generators," *IEEE Trans. on Energy Conversion*, vol. EC-1, no. 1, pp. 17-25, March 1986.

[9] M. M. Saied, "Matching of dc motors to photovoltaic generators for maximum daily gross mechanical energy," *IEEE Trans. on Energy Conversion*, vol. EC-3, no. 3, pp. 465-472, September 1988.

[10] J. Appelbaum, "The operation of loads powered by separate sources or by a common source of solar cells," *IEEE Trans. on Energy Conversion*, vol. EC-4, no. 3, pp. 351-357, September 1989.

[11] J. Appelbaum and M. S. Sarma, "The operation of permanent magnet dc motors powered by a common source of solar cells," *IEEE Trans. on Energy Conversion*, vol. EC-4, no. 4, pp. 635-642, December 1989.

[12] Z. Zinger, and A. Braunstein, "Dynamic matching of a solar-electrical (photovoltaic) system - An estimation of the minimum requirements on the matching system," *IEEE Trans. Power Apparatus and Systems*, vol. PAS-100, no. 3, pp. 1189-1192, March 1981.

[13] S. M. Alghuwainem, "Application of a dc chopper to maximize utilization of solar-cell generators," Paper 91 WM 145-3 EC, 1991 *IEEE/PES* 1991 Winter Meeting, New York, New York, Feb. 3-7, 1991.

[14] M. M. Saied, A. A. Hanafy, et al., "Optimal design parameters for a PV array coupled to a dc motor via a dc-dc transformer," *IEEE Trans. on Energy Conversion*, vol. EC-6, no. 4, pp. 593-598, December 1991.

[15] S. M. Alghuwainem, "Steady-state performance of dc motors supplied from photovoltaic generators with a step-up converter," *IEEE Trans. on Energy Conversion*, vol. EC-7, no. 2, pp. 267-272, June 1992.

[16] S. M. Alghuwainem, "Matching of dc motor to a photovoltaic generator using a step-up converter with a current-locked loop," Paper 93 SM 568-6 EC, presented at the *IEEE/PES* 1993 Summer Meeting, Vancouver, B.C., Canada, July 18-22, 1993.

Saad M. Alghuwainem received B.Sc. in Electrical Engineering from University of Riyadh in 1974. From 1974 to 1976 he worked as a teaching assistant in the EE Department, Riyadh University. He received M.Sc. degree in Electrical Engineering (Power) from University of Colorado, Boulder in 1978. From 1979 to 1981 he worked in the EE Department, King Saud University as a research assistant. From 1982 to 1986 he attended The University of Michigan, Ann Arbor where he received Ph.D. in Electrical Engineering. Since 1986 he has been with the Department of Electrical Engineering, King Saud University, where he is currently an associate professor. His interests include renewable energy sources, energy conversion systems, power system protection, and electromagnetic transients.